A novel phasor control design method: application to MEMS gyroscopes

Fabricio Saggin, Gérard Scorletti, Anton Korniienko

A novel phasor control design method: application to MEMS gyroscopes

Fabrício Saggin, Gérard Scorletti and Anton Korniienko

***Abstract*— In several applications, the main objective of the controllers is to ensure some process variable to track (and/or reject) a sinusoidal reference (disturbance) signal. To that end, two control approaches are defined: those based on the sinusoidal signals, and those based on the envelope (amplitude and phase) of these signals. The former one, which we name direct approach, corresponds to the classical architectures used in control engineering. This approach offers a broad range of methods to design linear controllers with guarantees of stability and performance. In general, envelope-based approaches are nonlinear and do not provide those guarantees. However, they allow obtaining controllers with a bandwidth much smaller than it would have in the direct approach. In this paper, we use time-varying complex phasors to describe the envelopes of the signals in the system. Then, we show that with a suitable reformulation, the system remains linear. Hence, links between these approaches are established under the assumption that a phasor can be instantaneously defined from a modulated signal (ideality). We propose thus two methods to design a phasor-based controller: one considering the ideal case and another where nonidealities are taken into account. Numerical examples, based on the operation of MEMS gyroscopes, show the effectiveness of these methods.**

I. Introduction

In numerous applications, the primary objective of a controller is to compute a control signal such that the output y of a (linear) process follows a sinusoidal reference trajectory y_r with a given frequency and/or reject sinusoidal disturbances with the same frequency. An emerging application illustrating this is the control of micro-electro-mechanical systems (MEMS) gyroscopes, where a proof mass shall oscillate close to the resonance frequency with a controlled amplitude, such that the angular rate can be accurately estimated [1], [2]. Similar examples are found in other fields, as in electrical machines and systems, inertial sensors, radio-frequency accelerators, see *e.g.* [3], [4], [5] and references therein.

In the literature, we may distinguish two main approaches to achieve the goals above for linear time-invariant (LTI) systems: the direct control, and the envelope or phasor-based one. The direct control corresponds to the general practice in control engineering: the control signal u is computed from the measurements of the plant output y and a sinusoidal reference signal y_r, as in [6], [7]. In this case, the controller can be designed by different methods, *e.g.* the H_∞ synthesis.

In the phasor-based approach, the control signal is often based on the envelope, *i.e.*, the amplitude and phase shift, of the signals of interest. The main advantage of this approach is that the envelope of the signals of interest are constant in steady-state. Hence, one can use, for instance, PID controllers to track the reference amplitude and phase shift, as in [8]. Another advantage is that the controller may work at a lower frequency than it would have in the classical architecture. Thus, in case of digital implementation, smaller sampling frequencies can be used. For these (implementation) reasons, this approach is widely used, for instance, in the control of MEMS gyroscopes [9]. Nevertheless, an important drawback of the envelope-based approach is that nonlinearities are included into the loop to compute the amplitude and phase shift of the signals. The conventional approach is then to linearize the system around operating points [1], [10], leading to controllers whose performance is not guaranteed.

In this paper, we show that by changing the signal representation, a complex-valued linear model is obtained. This modification is made by using the real and imaginary parts of a time-varying complex phasor, described in [3], instead of amplitude and phase shift representation. Even if the model becomes complex-valued, this reformulation allows us to design linear controllers with guarantees on the performance of the closed-loop system.

In this paper, we also reveal that there exists a link between the classical approach and the phasor one. This link allows transforming a controller designed for the direct approach into a controller for the phasor one, yielding the same performance level. Hence, linear controllers from the direct approach may be transposed to the phasor one. The only condition for this property to hold is that the phasor construction block is ideal, *i.e.*, a phasor can be instantaneously defined from a modulated/sinusoidal signal.

In practice, however, nonidealities are present in that construction block and may yield to a significant performance discrepancy and even instability of the closed-loop system. Another contribution of this paper is, therefore, a control design method, based on the H_∞ synthesis [11], that takes into account these nonidealities to compute a phasor-based controller, ensuring the stability and an appropriate performance level.

This paper is structured as follows. Section II states the phasor control problem. Section III presents the (linear) complex phasor model of an LTI system and some of its properties. In Section IV, links between the direct and the phasor approach are established, allowing to design a phasor-based controller from a direct one. Section V discusses how to implement the phasor construction block and the

The authors are with the Ampère Laboratory, UMR CNRS 5005, Ecole Centrale de Lyon, Université de Lyon, Ecully, France, fabricio.saggin@ec-lyon.fr

nonidealities entailed by it. Then, a novel phasor control design approach is presented, allowing one to take into consideration those nonidealities. Numerical examples, based on MEMS gyroscope operation, illustrate our main results in Section VI and conclusions are drawn in Section VII.

Notation: Subscripts R and I indicate respectively the real and imaginary parts of a complex variable; $j^2 = -1$. I_n is the identity matrix of $\mathbb{R}^{n\times n}$ and $0_{n\times m}$ is the zero matrix of $\mathbb{R}^{n\times m}$ (subscripts are omitted if obvious from context). For two matrices A, B, $\mathrm{diag}(A,B)$ is their diagonal concatenation. A^T is the transpose of A. $M_\perp$ denotes the orthogonal complement of M. In linear matrix inequalities (LMI), $\diamond$ represents terms that can be deduced from symmetry. For a complex matrix M, $\overline{\sigma}(M)$ denotes its maximum singular value. The $\star$ denotes the Redheffer (star) product [11]. For a given LTI system F, $\|F\|_\infty$ denotes its H_∞-norm. The L_2-norm of a signal v from $\mathbb{R}^+$ to $\mathbb{R}^{n_v}$ is defined as $\|v\|_2^2 = \int_0^\infty v(t)^T v(t)\mathrm{d}t$ and the set of signals for which the L_2-norm is bounded is denoted L_2. The L_2-gain of an operator Σ is defined as $\|\Sigma\|_{i2} = \sup_{v\in L_2,\, v\neq 0} \|\Sigma v\|_2/\|v\|_2$.

II. Phasor control problem

Let us consider the linear time-invariant (LTI) plant

$$G:\ \begin{cases} \dot{x}(t) = Ax(t) + Bu(t) \\ y(t) = Cx(t) + Du(t) \end{cases} \tag{1}$$

with $x(t)\in\mathbb{R}^n$, $u(t)\in\mathbb{R}^{n_u}$, $y(t)\in\mathbb{R}^{n_y}$, and real matrices A, B, C and D of appropriate dimensions. The original control objective is to compute u such that y tracks a sinusoidal reference y_r with frequency ω_0 and/or reject sinusoidal disturbances with the same frequency.

In control theory, this problem is usually solved by designing an LTI controller using, for instance, the H_∞ synthesis, see [11]. This controller computes u from the measurement of y and the reference y_r. We name this approach **direct control problem**.

An alternative approach, named **phasor control problem**, is considered. In this case, the control signal has the form:

$$u(t) = U(t)\cos\left(\phi_{exc}(t) + \phi_u(t)\right), \tag{2}$$

where $\phi_{exc}(t)$, called the excitation phase, is a given differentiable function. The couple (U, ϕ_u) is referred to as a phasor of the signal u, from where a complex phasor can be similarly defined: $\underline{u}(t) = U(t)e^{j\phi_u(t)}$. Then, instead of computing u, the controller K_{ph} computes U and ϕ_u from the measurement of Y and ϕ_y, similarly defined as:

$$y(t) = Y(t)\cos\left(\phi_{exc}(t) + \phi_y(t)\right), \tag{3}$$

that is the measure of the phasor of y. The control problem is then recast as the tracking and/or the rejection of phasor signals: compute the phasor (U, ϕ_u) such that the defined phasor (Y, ϕ_y) tracks a reference phasor (Y_r, ϕ_{y_r}).

The above description is illustrated in Fig. 1. The nonlinear block p2s transforms a phasor into a modulated signal, as in (2), and s2p transforms a modulated signal into a phasor (amplitude and phase shift) with respect to ϕ_{exc}.

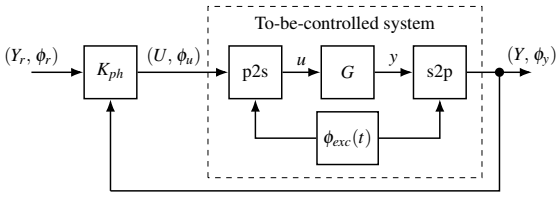

Fig. 1. Block-diagram of the phasor-based control architecture.

In the phasor control problem, the to-be-controlled plant is defined by (1), (2) and s2p, *i.e.*, (dropping time dependency)

$$\begin{cases} \dot{x} &= Ax + BU\cos\left(\phi_{exc} + \phi_u\right) \\ \begin{bmatrix} Y \\ \phi_y \end{bmatrix} &= \mathrm{s2p}\left(Cx + DU\cos\left(\phi_{exc} + \phi_u\right)\right) \end{cases}. \tag{4}$$

Since s2p and (2) are nonlinear functions of the phasor, the design of the controller is, a priori, a difficult problem. In the next section, we reveal that if the signals are replaced by their *complex* phasor, the plant (4) becomes linear.

III. Complex phasor modeling

A. Complex phasor model

The following theorem introduces a (linear) model of the plant based on the complex phasors.

Theorem 1. *Given a differentiable function $\phi_{exc}(t)$ and a couple (U, ϕ_u), the output y of the system* (1)*, for $u(t) = U(t)\cos\left(\phi_{exc}(t) + \phi_u(t)\right)$, is given by*

$$y(t) = Y(t)\cos\left(\phi_{exc}(t) + \phi_y(t)\right),$$

where (Y, ϕ_y) is such that $Y(t) = |\underline{y}(t)|$, $\phi_y(t) = \arg(\underline{y}(t))$ and $\underline{y}$ is the output of the system $\underline{G}$, defined by

$$\underline{G}:\ \begin{cases} \dot{\underline{x}}(t) &= \left(A - j\dot{\phi}_{exc}(t)I_n\right)\underline{x}(t) + B\underline{u}(t) \\ \underline{y}(t) &= C\underline{x}(t) + D\underline{u}(t) \end{cases} \tag{5}$$

for the input $\underline{u}(t) = U(t)e^{j\phi_u(t)}$.

Proof. Let $\underline{y}(t)$ and $\underline{x}(t)$ be solutions of (5) for the input $\underline{u}(t) = U(t)e^{j\phi_u(t)}$. By multiplying (5) by $e^{j\phi_{exc}(t)}$, we have, after simplifications

$$\begin{cases} \frac{d}{dt}\left(\underline{x}(t)e^{j\phi_{exc}(t)}\right) &= A\underline{x}(t)e^{j\phi_{exc}(t)} + B\underline{u}(t)e^{j\phi_{exc}(t)} \\ \underline{y}(t)e^{j\phi_{exc}(t)} &= C\underline{x}(t)e^{j\phi_{exc}(t)} + D\underline{u}(t)e^{j\phi_{exc}(t)} \end{cases}.$$

By taking the real part, since A, B, C and D are real-valued matrices, we obtain

$$\begin{cases} \frac{d}{dt}\left(\Re\left(\underline{x}e^{j\phi_{exc}}\right)\right) &= A\Re\left(\underline{x}e^{j\phi_{exc}}\right) + B\Re\left(\underline{u}e^{j\phi_{exc}}\right) \\ \Re\left(\underline{y}e^{j\phi_{exc}}\right) &= C\Re\left(\underline{x}e^{j\phi_{exc}}\right) + D\Re\left(\underline{u}e^{j\phi_{exc}}\right) \end{cases}.$$

This system corresponds to (1) when the input signal is given by $u(t) = U(t)\cos\left(\phi_{exc}(t) + \phi_u(t)\right)$. □

Note that the system $\underline{G}$, see (5), computes the complex phasors of x and y from the complex phasor of the input u. Thus, $\underline{G}$ is referred to as the Complex Phasor Model (CPM) of G. Furthermore, $\underline{G}$ is linear parameter varying (LPV). However, when $\phi_{exc}(t) = \omega_0 t$, it is actually an LTI system.

The CPM is a system with complex-valued parameters. Nonetheless, by splitting the signals into real and imaginary parts, $\underline{G}$ is equivalently represented by the real-valued system below, denoted Complex Phasor Real Model (CPRM):

$$G_{cp}: \begin{cases} \dot{x}_{cp}(t) = A_{cp}\left(\dot{\phi}_{exc}(t)\right)x_{cp}(t) + B_{cp}u_{cp}(t) \\ y_{cp}(t) = C_{cp}x_{cp}(t) + D_{cp}u_{cp}(t) \end{cases} \tag{6}$$

with $x_{cp} = [\underline{x}_R^T \ \underline{x}_I^T]^T$, $u_{cp} = [\underline{u}_R^T \ \underline{u}_I^T]^T$, $y_{cp} = [\underline{y}_R^T \ \underline{y}_I^T]^T$,

$$A_{cp}\left(\dot{\phi}_{exc}(t)\right) = \begin{bmatrix} A & \dot{\phi}_{exc}(t)I_n \\ -\dot{\phi}_{exc}(t)I_n & A \end{bmatrix},$$

$B_{cp} = \mathrm{diag}(B,B)$, $C_{cp} = \mathrm{diag}(C,C)$ and $D_{cp} = \mathrm{diag}(D,D)$. Note that this model corresponds to

$$\begin{cases} \dot{x} = Ax + B\begin{bmatrix}\cos(\phi_{exc}) & -\sin(\phi_{exc})\end{bmatrix}u_{cp} \\ y_{cp} = \mathrm{s2cp}\left(Cx + D\begin{bmatrix}\cos(\phi_{exc}) & -\sin(\phi_{exc})\end{bmatrix}u_{cp}\right) \end{cases}, \tag{7}$$

where x is the state vector of (4) and s2cp is an operator that associates y_{cp} with y.

Based on the CPRM, we define a new control problem, named **complex phasor control problem**. In this problem, the plant is defined by G_{cp} of (6); the controller, denoted K_{cp}, has to compute u_{cp} from y_{cp} and $y_{r_{cp}}$ such that y_{cp} tracks the reference signal $y_{r_{cp}}$.

For the sake of simplicity, in this work, we focus on the case where $\phi_{exc}(t) = \omega_0 t$, *i.e.*, G_{cp} is an LTI system. The general case can be similarly discussed using the LPV control approach, see *e.g.* [12].

Before to proceed with the solution for the complex phasor control problem, we present some relevant properties of the complex phasor model in the LTI case.

B. Properties of the complex phasor model in the LTI case

The systems $\underline{G}$ and G_{cp} have poles with the same real part that the poles of G. Then, the stability of one is equivalent to the stability of the others. Moreover, since $\underline{G}$ can be defined as $\underline{G}(s) = G(s + j\omega_0)$, the frequency response of $\underline{G}$ corresponds to a frequency shift of the frequency response of G. Thus, $\|G(s)\|_\infty = \|\underline{G}(s)\|_\infty = \left\|G_{cp}(s)\right\|_\infty$ [5].

IV. Control design based on the direct problem

In this section, we intend to answer two key questions.

(i) Besides the implementation-related advantages of phasor control approach over the direct control one [9], does any of them ensure a better performance level?

(ii) Is it possible to compute a direct controller and transform it into a complex phasor controller?

We define the performance level as an upper bound on the H_∞-norm of the interconnection of the augmented plant, *i.e.*, the plant augmented with weighting functions, and the controller [11].

A. Solving the direct control problem and the complex phasor control problem

The controller for the direct control problem can be computed by solving the standard H_∞ problem. We consider an augmented plant P, composed of the plant G and weighting functions, usually defined by a state-space representation

$$P: \begin{cases} \dot{x}_P &= A_P x_P &+ B_u u_P &+ B_w w \\ y_P &= C_y x_P & &+ D_{yw} w \\ z &= C_z x_P &+ D_{zu} u_P &+ D_{zw} w \end{cases} \tag{8}$$

with $x_P(t) \in \mathbb{R}^{n_P}$, $u_P(t) \in \mathbb{R}^{n_{u_P}}$, $w(t) \in \mathbb{R}^{n_w}$, $y_P(t) \in \mathbb{R}^{n_{y_P}}$, $z(t) \in \mathbb{R}^{n_z}$, and real matrices of appropriate dimensions. The problem is: given $\gamma > 0$, compute a controller

$$K: \begin{cases} \dot{x}_K &= A_K x_K &+ B_K y_P \\ u_P &= C_K x_K &+ D_K y_P \end{cases}, \tag{9}$$

where $x_K(t) \in \mathbb{R}^{n_P}$, if there is any, such that $\|P \star K\|_\infty < \gamma$, *i.e.*, the closed-loop system defined by (8) and (9) has an H_∞ norm smaller than γ. The feasibility of this problem is assessed by the following theorem.

Theorem 2 ([13])**.** *Consider the system* (8)*. Then, there is a dynamic output feedback, in the form of* (9)*, such that $\|P \star K\|_\infty < \gamma$ if and only if there exist $R, S \in \mathbb{R}^{n_P \times n_P}$ such that $R = R^T$, $S = S^T$,*

$$\begin{bmatrix}\diamond\end{bmatrix}_\perp^T \begin{bmatrix} SA_P^T + A_P S & B_w & SC_z^T \\ B_w^T & -\gamma I & D_{zw}^T \\ C_z S & D_{zw} & -\gamma I \end{bmatrix} \begin{bmatrix} B_u^T & 0 & D_{zu}^T \end{bmatrix}_\perp \prec 0,$$

$$\begin{bmatrix}\diamond\end{bmatrix}_\perp^T \begin{bmatrix} A_P^T R + RA_P & RB_w & C_z^T \\ B_w^T R & -\gamma I & D_{zw}^T \\ C_z & D_{zw} & -\gamma I \end{bmatrix} \begin{bmatrix} C_y & D_{yw} & 0 \end{bmatrix}_\perp \prec 0$$

$$\text{and} \quad \begin{bmatrix} R & I \\ I & S \end{bmatrix} \succ 0.$$

The complex phasor control problem can be addressed as a special case of the H_∞ control problem, but with an augmented plant P_{cp}, which is the CPRM associated to P. Nevertheless, the solution $\underline{K}$ of this H_∞ control problem does not necessarily admit a state-space representation with the structure of a CPRM.

Since the direct control problem and the complex phasor one can be formulated as H_∞ control problems, we consider this formalism to investigate the links between them.

B. Connections between the direct control problem and the complex phasor real control problem

We now investigate the connections between the direct control problem and the complex phasor one.

Theorem 3. *Let P be the plant defined in* (8) *and K the controller defined by* (9)*. Let P_{cp} and K_{cp} be respectively the CPRM of P and K for $\phi_{exc}(t) = \omega_0 t$. Hence, given $\gamma > 0$,*

1) *if K is such that $\|P \star K\|_\infty < \gamma$, then $\|P_{cp} \star K_{cp}\|_\infty < \gamma$;*
2) *$(P \star K)_{cp} = P_{cp} \star K_{cp}$;*
3) *there exists a controller $\underline{K}$ such that $\|P_{cp} \star \underline{K}\|_\infty < \gamma$ if and only if there exists K such that $\|P \star K\|_\infty < \gamma$.*

Proof. Here, we just present the sketch of the proof. Details for the property 3 are developed in [14], and, for the sake of briefness, the details based on routine algebra are omitted.

Properties 1) & 2): By building the state-space realizations of $(P \star K)_{cp}$ and $P_{cp} \star K_{cp}$ from those of P and K and by

observing that they are equal, we prove the property 2. From section III-B, $\|(P\star K)_{cp}\|_\infty = \|P\star K\|_\infty$, then $\|P\star K\|_\infty = \|P_{cp}\star K_{cp}\|_\infty$, which proves property 1.

Property 3): The proof consists in first applying the H_∞ problem associated to the complex phasor control problem. The existence of $\underline{K}$ such that $\|P_{cp}\star\underline{K}\|_\infty < \gamma$ is equivalent to the fact that the feasibility problem defined by Theorem 2 has a solution. The second step consists in using the solution of this feasibility problem to construct the solution of the feasibility problem defined by Theorem 2 when this theorem is applied to the direct control problem, which implies that there exists K such that $\|P\star K\|_\infty < \gamma$. □

The first property claims that if a direct controller K achieves a performance level γ, then K_{cp} is a solution of the complex phasor control problem, ensuring the same performance level. The second property states that the complex phasor model of the interconnection $P\star K$ is equal to the interconnection of each complex phasor model.

The third property reveals that if a solution $\underline{K}$ of the complex phasor control problem achieves a given performance level, then, necessarily, the same level of performance can be obtained by a direct controller and vice-versa. In other words, even with an augmented degree of freedom (number of variables), the complex phasor control cannot ensure better performance level than that of the direct control.

All these results are based on the fact that (7) is exactly described by G_{cp}. However, the (ideal) s2cp block cannot be implemented. To extract amplitude and phase of a signal (or real and imaginary parts), additional nonlinear operators and filters are introduced into the loop. These elements, that were not considered in this section, may deteriorate the performance of the closed-loop system or even make it unstable. In the sequel, we discuss how to implement the s2cp block and how to model its nonidealities. Then, we propose an approach to take into account these nonidealities during the control design.

V. Implementation of s2cp and control design

Up to this point, we have considered the s2cp block as an operator that allows to extract y_{cp} from a signal y. Nonetheless, by observing (3), one can notice that, for a given ϕ_{exc} and y, an infinity number of couples (Y,ϕ_y), and consequently $(\underline{y}_R,\underline{y}_I)$, satisfies the equation. This ambiguity problem is recurrent in communication theory and signal processing, and can be solved by means of the Hilbert transform [15]. In practice, this operation is performed by a synchronous demodulation, introducing constraints on the signals and nonidealities into the s2cp block. In this section, we discuss the implementation of the s2cp block and how to model its nonidealities. Then, we propose a control design method that takes them into account.

A. Implementation of the s2cp block

In practice (with $\phi_{exc}(t)=\omega_0 t$), the operator s2cp is implemented by a synchronous demodulation if the power spectrum of y is in the interval $(0,2\omega_0)$ [15]. Fig. 2 shows

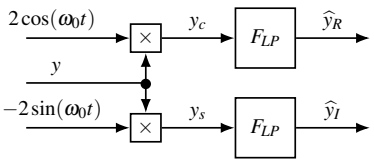

Fig. 2. Block-diagram of the synchronous demodulation.

the scheme of the demodulator, which includes **ideal** low-pass filters F_{LP} with cutoff frequency $\omega_c=\omega_0$. This scheme is motivated by the following point. Let $\underline{y}$ be the complex phasor of y, *i.e.*, $y(t)=\underline{y}_R(t)\cos(\omega_0 t)-\underline{y}_I(t)\sin(\omega_0 t)$. Then, $y_c(t)=2y(t)\cos(\omega_0 t)$ and $y_s(t)=-2y(t)\sin(\omega_0 t)$ are recast:

$$\begin{aligned} y_c(t) &= \underline{y}_R(t) + \overbrace{\left(\underline{y}_R(t)\cos(2\omega_0 t)-\underline{y}_I(t)\sin(2\omega_0 t)\right)}^{\delta\underline{y}_R(t)} \\ y_s(t) &= \underline{y}_I(t) - \underbrace{\left(\underline{y}_R(t)\sin(2\omega_0 t)+\underline{y}_I(t)\cos(2\omega_0 t)\right)}_{\delta\underline{y}_I(t)} \end{aligned} \tag{10}$$

As the power spectrum support of the signal y is assumed to be included in the frequency interval $(0,2\omega_0)$, the power spectrum support of $\underline{y}_R(t)$ and $\underline{y}_I(t)$ is in $(0,\omega_0)$, and the power spectrum support of $\delta\underline{y}_R(t)$ and $\delta\underline{y}_I(t)$ is in $(\omega_0,3\omega_0)$. As a consequence, since F_{LP} is an ideal filter with $\omega_c=\omega_0$, $\widehat{y}_R(t)=\underline{y}_R(t)$ and $\widehat{y}_I(t)=\underline{y}_I(t)$.

In practice, the low-pass filters are not ideal. Indeed, they present a transition band between the pass band and the stop band. Since the power spectrum support of $\delta\underline{y}_R(t)$ and the power spectrum support of $\underline{y}_R(t)$ can be very close, the existence of the transition band can dramatically change the behavior of the closed-loop system. Then, it is crucial to:

1) evaluate the effect of this nonideal filter when the controller was computed as described in section IV; this *a posteriori* analysis is investigated in [9];
2) consider this nonideality when designing the control law; this point is developed in the sequel.

B. Modeling the nonidealities of s2cp

The question now is how to model the nonideal s2cp. From (10), y_c and y_s can be rewritten in matrix form as

$$\begin{bmatrix} y_c(t) \\ y_s(t) \end{bmatrix} = (I+\Delta(\omega_0))\begin{bmatrix} \underline{y}_R(t) \\ \underline{y}_I(t) \end{bmatrix}$$

$$\text{with} \qquad \Delta(\omega_0)=\begin{bmatrix} \cos(2\omega_0 t) & -\sin(2\omega_0 t) \\ -\sin(2\omega_0 t) & -\cos(2\omega_0 t) \end{bmatrix}.$$

Then, the nonideal s2cp (synchronous demodulation) is modeled as the series connection of an ideal s2cp, the block $(I+\Delta(\omega_0))$ and the nonideal filters F_{LP}, as in Fig. 3. In the sequel, this modeling is used to compute a CPRM controller.

C. Solution to the complex phasor control problem with nonideal s2cp

Here, we briefly present how to compute a controller which ensures performance and robust stability with respect to the nonidealities of s2cp using H_∞ criterion.

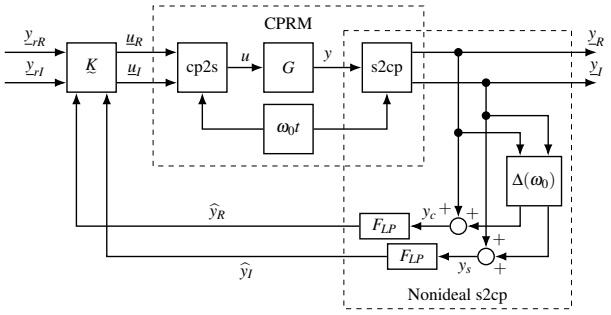

Fig. 3. Scheme of the complex phasor architecture with nonideal s2cp.

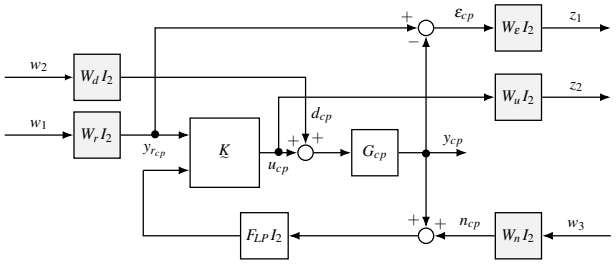

Fig. 4. Considered criterion for the H_∞ synthesis.

Based on the H_∞ synthesis [11], the solution is obtained by finding $\underline{K}$, if there is any, such that

$$\left\| \begin{matrix} W_\varepsilon T_{y_{rcp}\to\varepsilon_{cp}} W_r & W_\varepsilon T_{d_{cp}\to\varepsilon_{cp}} W_d & W_\varepsilon T_{n_{cp}\to\varepsilon_{cp}} W_n \\ W_u T_{y_{rcp}\to u_{cp}} W_r & W_u T_{d_{cp}\to u_{cp}} W_d & W_u T_{n_{cp}\to u_{cp}} W_n \end{matrix} \right\|_\infty < 1, \quad (11)$$

where $W_n(s) = W_\varepsilon(s)^{-1}$, $T_{a\to b}$ denotes the transfer from signal a to signal b, and scalar weighting functions W_i, with $i \in \{r, d, n, \varepsilon, u\}$, express the control specifications, detailed in the report [14]. This H_∞ criterion is shown in Fig. 4.

Concerning the nonideal s2cp, note that (11) implies $\|W_\varepsilon T_{n_{cp}\to\varepsilon_{cp}} W_n\|_\infty < 1$. Moreover, since $T_{n_{cp}\to\varepsilon_{cp}} = -T_{n_{cp}\to y_{cp}}$ and $W_n = {W_\varepsilon}^{-1}$, this inequality implies $\|T_{n_{cp}\to y_{cp}}\|_\infty < 1$. As the L_2 gain of an LTI system is equal to its H_∞ norm [16], the L_2 gain of $T_{n_{cp}\to y_{cp}}$ is strictly less than 1.

The system presented in Fig. 3 can be rewritten as the interconnection of $T_{n_{cp}\to y_{cp}}$ and $\Delta(\omega_0)$. Since $\forall\, t, \omega_0 \in \mathbb{R}$, $\overline{\sigma}(\Delta(\omega_0)) \leq 1$, the L_2 gain of the operator that associates y_{cp} with $\Delta(\omega_0) y_{cp}$ is equal to 1. Then, since the product of the L_2 gain of this operator and the L_2 gain of $T_{n_{cp}\to y_{cp}}$ is strictly less than 1, the stability of the overall interconnected system is obtained by applying the small gain theorem [16].

VI. Numerical examples

In this section, we illustrate the different control approaches of this paper. To this end, we consider the operation of a MEMS gyroscope, which is composed of a proof mass with two perpendicular resonant modes. Oscillations are driven on the so-called drive mode. Then, if the device is submitted to an angular rate perpendicular to those axes, due to the Coriolis effect, oscillations are produced on the so-called sense mode. By measuring these secondary oscillations, the actual angular rate can be estimated. The accuracy of the gyroscope depends (among other factors) on how well controlled are the oscillations on the drive mode [1], [10].

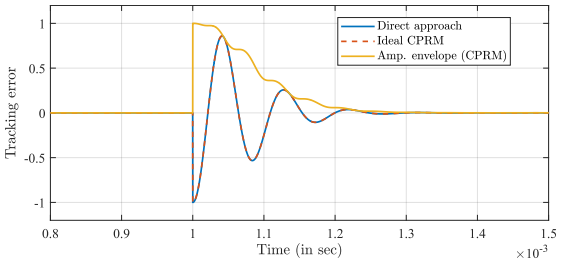

Fig. 5. Case 1 - comparison between the tracking errors of direct approach (G, K) and ideal CPRM $(G_{cp} K_{cp})$.

Thus, we focus on the control of the drive mode. For further details on the MEMS gyroscopes operation, see *e.g.* [1], [2].

The model of a MEMS gyroscope drive mode is given by (1) with $A = \begin{bmatrix} 0 & 1 \\ -\omega_n^2 & -\omega_n/Q \end{bmatrix}$, $B = \begin{bmatrix} 0 & \omega_n \end{bmatrix}^T$, $C = \begin{bmatrix} 1 & 0 \end{bmatrix}$, $D = 0$, $\omega_n = 2\pi \cdot 11500$ rad s^{-1} and $Q = 50$ [14]. Let us consider the following specifications:

1) tracking of a reference signal $y_r(t) = Y_r \cos(\omega_0 t)$ with $\omega_0 = \omega_n$ and an error $\varepsilon(t) = y_r(t) - y(t)$ such that $\forall t \geq 0.5$ ms, $|\varepsilon(t)| < 0.002 Y_r$;
2) the closed-loop system is stable, *i.e.* the stability against the nonidealities of the s2cp has to be guaranteed.

In the sequel, we consider two cases: *(i)* we design a controller in the direct approach and take its corresponding CPRM to apply in a phasor approach, as presented in section IV; *(ii)* we design a phasor controller taking the s2cp nonidealities into account, as discussed in section V.

Here, we discuss the main results. Details on the controller design and numerical values are available in [14].

A. Case 1: design based on the direct control problem

In this first case, we design a controller for the direct approach by solving the standard H_∞ problem. This controller is then transformed into a phasor controller K_{cp} via Theorem 1 and implemented according to the phasor-based architecture.

To evaluate the tracking performance of the obtained controller, we apply an amplitude reference step at $t = 1$ ms and $\omega_0 = \omega_n$. The closed loop composed of K and G is referred to as direct approach, whereas the (virtual) control loop composed by K_{cp} and G_{cp} is denoted ideal CPRM. Fig. 5 presents the tracking error of both strategies, which are superposed. We also observe that, in about 0.3 ms, the error converges to its steady-state value, which is close to $0.001 Y_r$. For the sake of illustration, we also present the amplitude envelope computed from the ideal CPRM, that corresponds to the amplitude of the tracking error. This fact illustrates the Theorem 1 and validates the discussions of section IV.

In order to evaluate the closed-loop system with the phasor control and the nonideal s2cp, we simulate the overall system (G, nonideal s2cp, K_{cp}, cp2s) with $F_{LP}(s) = \frac{\omega_c}{s+\omega_c}$ and $\omega_c = 2\pi \cdot 100$ rad s^{-1}. The simulation results are presented in Fig. 6, where we notice that the error has higher values and takes more than 20 ms to achieve steady-state. When in steady-state, the error amplitude is about $0.005 Y_r$. These

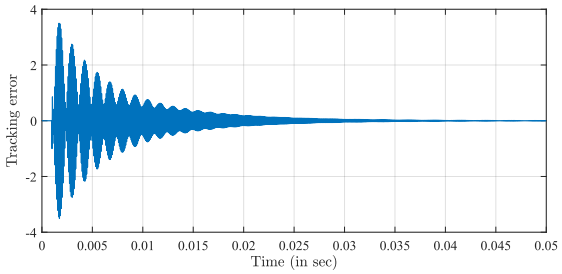

Fig. 6. Case 1 - tracking error of the nonideal CPRM (G, nonideal s2cp, K_{cp}, cp2s) with $\omega_c = 2\pi \cdot 100\,\mathrm{rad\,s^{-1}}$.

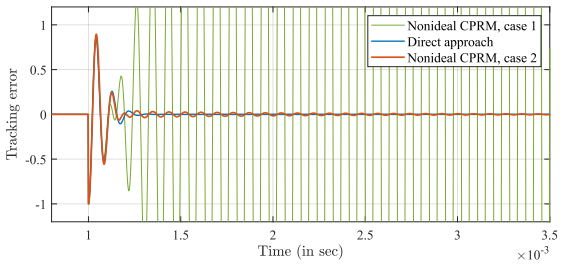

Fig. 7. Case 2 - comparison between direct approach and nonideal CPRM with $\omega_x = 2\pi \cdot 8\,\mathrm{rad\,s^{-1}}$ for case 1 (K_{cp}) and case 2 ($\tilde{K}$).

substantial differences with respect to the ideal CPRM are mainly due to F_{LP}, present in the nonideal s2cp.

Besides the important changes on the behavior of the closed-loop system, if we reduce the cutoff frequency of F_{LP}, the system may become unstable. This is the case when we make, *e.g.*, $\omega_c = 2\pi \cdot 8\,\mathrm{rad\,s^{-1}}$, illustrated in Fig. 7.

B. Case 2: design based on the CPRM and nonideal s2cp

Here, we illustrate the method presented in section V. We consider F_{LP} with $\omega_c = 2\pi \cdot 8\,\mathrm{rad\,s^{-1}}$, which makes the closed-loop system of the previous case unstable.

With the H_∞ synthesis, we obtain a controller that ensures, in addition to the reference tracking, $\|T_{n_{cp} \to y_{cp}}\|_\infty = 0.983$. Hence, the small gain theorem conditions are satisfied and ensure the stability of the closed-loop system in presence of the time-varying matrix $\Delta(\omega_0)$.

The overall system (G, nonideal s2cp, $\underline{K}$, cp2s) is simulated with $\omega_c = 2\pi \cdot 8\,\mathrm{rad\,s^{-1}}$. We apply the same reference signal of the previous case. The tracking error is presented in Fig. 7. For the sake of comparison, we also plot the results with the controller designed in case 1 (instability) and direct approach. We observe that, despite the nonideal s2cp, at the transient-state, the phasor controller that takes F_{LP} into account (case 2) has a performance similar to the direct one. The phasor approach presents some small oscillations until $t \approx 3\,\mathrm{ms}$. In steady-state, the tracking errors of both strategies converge to close to $0.001 Y_r$, as required. Furthermore, note that the phasor controller is conceived to control the nonlinear system presented in Fig. 1 or Fig. 3, where a direct controller cannot be applied.

VII. Conclusions

In some application, as the control of MEMS gyroscopes, it is usual to consider a phasor control architecture due to its implementation advantages. However, this strategy introduces nonlinear elements into the loop. In this paper, we present the complex phasor modeling, which allows considering the to-be-controlled system as linear for the controller design.

Correspondences between classical control architectures and phasor-based ones were established. These equivalences allow one to design a linear controller in classical architecture and implement an equivalent controller in a phasor-based architecture, ensuring the same performance level if the s2cp block is ideal. In practical implementations, nonidealities appear and can quickly degrade the performance of the closed-loop system. The modeling of these nonidealities allows us to analyze the closed-loop system and to take them into account to design a controller. Simulation results emphasized the effectiveness of the proposed method.

The final message of this paper is that if there are practical constraints imposing the use of a phasor architecture, the nonidealities of the s2cp block have to be taken into consideration, guaranteeing that the design specifications are verified in the real implementation.

References

[1] M. Saukoski, "System and circuit design for a capacitive MEMS gyroscope," Ph.D. dissertation, Helsinki University of Technology, 2008.

[2] V. Kempe, *Inertial MEMS - principles and practice*. Cambridge: Cambridge University Press, 2011.

[3] V. Venkatasubramanian, "Tools for dynamic analysis of the general large power system using time-varying phasors," *Int. J. Electr. Power Energy Syst.*, vol. 16, no. 6, pp. 365–376, 1994.

[4] B. Boivin, P. Coirault, L. Rambault, and N. Maamri, "Modelling and H_∞ controller applied to a gyrometer," in *IEEE Int. Conf. Syst. Man Cybern.*, vol. 4. IEEE, 2002, p. 6.

[5] O. Troeng, B. Bernhardsson, and C. Rivetta, "Complex-coefficient systems in control," in *Am. Control Conf.*, no. 4. IEEE, may 2017, pp. 1721–1727.

[6] M. H. Pishrobat and J. Keighobadi, "Model predictive control of MEMS vibratory gyroscope," *IFAC Proc.*, vol. 47, no. 3, pp. 7278–7283, 2014.

[7] M. Rahmani, "MEMS gyroscope control using a novel compound robust control," *ISA Trans.*, vol. 72, pp. 37–43, jan 2018.

[8] Zurich Instruments, "Control of MEMS Coriolis Vibratory Gyroscopes," Zurich Instruments, Tech. Rep. October, 2015. [Online]. Available: https://www.zhinst.com/sites/default/files/zi_appnote_mems_gyroscope.pdf

[9] J. Ayala-Cuevas, F. Saggin, G. Scorletti, and A. Korniienko, "Stability Analysis of Time-Varying Systems with Harmonic Oscillations Using IQC Frequency Domain Multipliers," in *Proc. IEEE Conf. Decis. Control*, 2019.

[10] M. Egretzberger, F. Mair, and A. Kugi, "Model-based control concepts for vibratory MEMS gyroscopes," *Mechatronics*, vol. 22, no. 3, pp. 241–250, Apr. 2012.

[11] S. Skogestad and I. Postlethwaite, *Multivariable feedback control - analysis and design*, 2nd ed. John Wiley & Sons, 2001.

[12] G. Scorletti and L. E. Ghaoui, "Improved LMI conditions for gain scheduling and related control problems," *Int. J. Robust Nonlin.*, vol. 8, no. 10, pp. 845–877, 1998.

[13] P. Gahinet, "Explicit controller formulas for LMI-based H_∞ synthesis," *Automatica*, vol. 32, no. 7, pp. 1007–1014, jul 1996.

[14] F. Saggin, G. Scorletti, and A. Korniienko, "On Phasor Control for Linear Time Invariant Systems," Ecole Centrale Lyon, Techincal Report, Mar. 2019. [Online]. Available: https://hal.archives-ouvertes.fr/hal-02068370

[15] D. Vakman, "On the analytic signal, the Teager-Kaiser energy algorithm, and other methods for defining amplitude and frequency," *IEEE Trans. Signal Process.*, vol. 44, no. 4, pp. 791–797, apr 1996.

[16] M. Vidyasagar, *Nonlinear systems analysis*, 2nd ed. Englewood Cliffs, NJ: Prentice Hall, 2002.